JGR Atmospheres

RESEARCH ARTICLE
10.1029/2019JD031874

Subseasonal Variability of Elevated Dust Concentrations Over South Florida

S. J. Kramer[1], B. P. Kirtman[1], P. Zuidema[1], and F. Ngan[2]

[1]Rosenstiel School of Marine and Atmospheric Science, University of Miami, Miami, FL, USA, [2]NOAA/Air Resource Laboratory and Cooperative Institute for Satellite Earth System Studies, University of Maryland, College Park, MD, USA

Key Points:
- Strengthened easterlies over the West Tropical Atlantic and southerly winds over the Florida Peninsula linked to high Saharan dust at Miami
- The North Atlantic subtropical high (NASH) is displaced southward and elongated to the west during these periods of favorable flow
- Newly defined dust transport efficiency correlates well with increases in dust mass concentrations at subseasonal and seasonal time scales

Supporting Information:
- Supporting Information S1
- Figure S1
- Figure S2
- Figure S3
- Figure S4
- Figure S5
- Figure S6
- Figure S7
- Figure S8
- Figure S9
- Figure S10
- Table S1

Correspondence to:
S. J. Kramer,
skramer@rsmas.miami.edu

Citation:
Kramer, S. J., Kirtman, B. P., Zuidema, P., & Ngan, F. (2020). Subseasonal variability of elevated dust concentrations over South Florida. *Journal of Geophysical Research: Atmospheres*, *125*, e2019JD031874. https://doi.org/10.1029/2019JD031874

Received 21 OCT 2019
Accepted 24 FEB 2020
Accepted article online 26 FEB 2020

Abstract Dust mass concentrations have been measured daily at Miami, Florida, in the summer months, and biweekly throughout the remaining months, since 1974. The 43-year record of dust mass concentrations indicate large daily, seasonal, and interannual variations, with most of the dust arriving within 5–8 episodes each summer. On average, dust arrives to Miami, Florida, 10 days after emission from North Africa, with measured concentrations depending on characteristics of the lower free-tropospheric winds due to the vast travel distance. Daily dust mass concentrations from July and August, the months that contribute the most to the annual mean, are used to characterize the synoptic conditions most favorable for dust transport. Two key regions are linked with the highest daily dust mass concentrations above Miami: (i) easterly winds, averaged over 850–500 mb, over the Tropical West Atlantic [15–25°N, 45–80°W], and (ii) southerly winds, similarly averaged, over the Florida Peninsula [20–30°N,75–80°W]. Winds within these two regions are enhanced when the North Atlantic subtropical high is displaced south and zonally elongated, relocating the western edge over Florida. A dust-transport-efficiency index, based on the maximum potential for dust to arrive above Miami with limited loss to deposition or mixing, identifies high-dust loading cases on the subseasonal scale. Monthly dust-transport-efficiency values agree well with the monthly dust trends over the 43-year time span. While seasonal dust loadings have been decreasing over Florida in the past decade, the transport efficiency has been increasing, possibly due to trends in the North Atlantic subtropical high.

Plain Language Summary Winds over the Saharan desert lift small dust particles into the air, which remain airborne for a few weeks, and slowly fall to the ground and ocean thousands of kilometers away. The dusty-air is carried across the Atlantic Ocean to Miami, Florida, during the summer months, disrupting hurricane development, cloud features, and affecting human health. Dust is measured at the Rosenstiel School of Marine and Atmospheric Science each summer day since 1974 and twice weekly in other seasons. We compare days with the largest and smallest measured values of dust in July and August to identify wind regions that are most important for bringing dusty-air, and what causes them to be stronger some years but not others. We located two regions of wind, which are critical for large amounts of dust to reach Miami: (i) east-to-west winds over the Tropical West Atlantic and (ii) south-to-north winds over the Florida Peninsula. By averaging the monthly wind speeds in the two critical regions, we can estimate the amount of dust which reaches Miami, Florida, each summer. This may improve future forecasts, warnings, and hurricane products.

1. Introduction

Saharan dust is transported within dry and stable air masses that propagate off the African coast, denoted Saharan Air Layers (SALs; Carlson & Prospero, 1972). The North African source region is the largest contributor to global dust (Ginoux et al., 2004; Huneeus et al., 2011; United Nations Environment Programme (UNEP) et al., 2016) and is the main aerosol contributor to the atmosphere above Miami, Florida, during boreal summer (Prospero, 1999a). Of the transported dust particles from the Sahara, almost 50% are less than 2.5 μm in diameter (Li-Jones & Prospero, 1998; Prospero et al., 2001; Prospero & Mayol-Bracero, 2013). Airborne particles with diameter less than 2.5 μm, termed particulate matter 2.5, pose a health risk for human lung tissue and are monitored by the U.S. Environmental Protection Agency (USEPA; Garrison et al., 2014). Through the absorbing and scattering of solar radiation, dust attenuates the solar flux reaching the surface resulting in cooler ocean surface

temperatures (Lau & Kim, 2007; Mahowald et al., 2014). The net radiative heating structure affects cloud cover at small scales and regional circulation patterns at larger scales. Dust particles can alter the microphysical cloud processes through serving as cloud condensation nuclei. Dust may also affect the diabatic heating within organized deep convection and act to hinder tropical cyclone development (Dunion & Velden, 2004; Zhang et al., 2007; Zipser et al., 2009).

Dust emission and transport are primarily controlled by synoptic meteorology, specifically pressure gradients, which induce strong winds over the Sahara and tropical Atlantic. Dust is lofted into the atmosphere by strong surface winds over the Sahara, associated with a low-level jet induced by a surface pressure gradient (Knippertz & Todd, 2012). During the summer, dusty Saharan air is episodically ejected off the African coast behind the trough of an African easterly wave disturbance and cutoff by marine air, which flows north with the ridge (Carlson & Prospero, 1972). The dusty-continental air is denoted a SAL, as the air mass has a distinctively higher temperature and an extremely low moisture in comparison to the surrounding marine air (Carlson & Prospero, 1972). A SAL has a defined border extending from inside the boundary layer up to 5 km (Tsamalis et al., 2013) and moves west as an independent air mass. The temperature gradient associated with the SAL enhances the easterly wave disturbance over the Atlantic due to the strong baroclinicity behind the trough and induces a thermal wind component inside the SAL (Carlson & Prospero, 1972; Karyampudi & Carlson, 1988). The SAL sinks slowly while traversing the Atlantic, and entrainment of air from outside the SAL layer acts to disperse the warm air and aid in dust particle mixing with marine air. The North Atlantic subtropical high (NASH) is the dominating circulation influence over the basin in the summer months, centered at 35°N, 40°W (Davis et al., 1997), and therefore likely of key importance to the strength of background easterly flow affecting dust transport. Reanalysis studies have found an intensification and western shift in the NASH when comparing 1978–2007 to 1948–1977 (L. Li, et al., 2011; W. Li, et al., 2011), which may influence dust variability over the observational record.

Despite the known synoptic dependence, interannual variability of dust loading follows a 5- to 8-year oscillatory pattern (Evan et al., 2016) that has not yet been explained. The relative effects of large-scale variability from climate signals such as El Niño Southern Oscillation (ENSO) and North Atlantic Oscillation (NAO) on emission or transport can be difficult to distinguish as it depends on which region the dust loadings are defined, either the source emissions or the loadings after some length of transport. Previous research has been inconclusive or contradictory when comparing interannual dust variability to known climate indices. A connection between the NAO and dust emission from the Sahara to the Atlantic and Mediterranean was found with a strong positive correlation to the Barbados dust record on a yearly basis (Chiapello & Moulin, 2002; Moulin et al., 1997). More recent correlations between the NAO and Barbados dust concentrations in the wintertime were nonexistent (Ginoux et al., 2004) or extremely small (Doherty et al., 2012). Connections between dust mass and ENSO have also been found but do not yet demonstrate consistency: a connection between peak dust years at Barbados and El Niño events was recognized (Prospero & Lamb, 2003), a small positive correlation between wintertime dust at Barbados to El Niño (Doherty et al., 2012), and a small positive correlation between summertime dust at Barbados during La Niña (DeFlorio et al., 2016). Unlike interannual variability, dust variability research focused on the decadal scale has shown consistency. Satellite-based aerosol optical depth emission estimates have also been declining over the last century (Evan et al., 2006; Ridley et al., 2014) consistent with climate model predictions (Evan et al., 2016).

We focus on the transport of Saharan dust to South Florida, which begins in May, peaks in July, and concludes in September. Saharan dust is the largest contributor to Miami's aerosol environment in the summer months, overtaking other natural and anthropogenic aerosols including sea salt, and has been measured at Miami, Florida [25.76°N, 80.19°W], since 1974 (Prospero, 1999a). This rare long-term record encompasses dust mass concentrations taken daily in the summer months [June, July, August, and September] and biweekly measurements during the remaining months. We utilize the 43-year daily in situ record to analyze July and August, the two largest contributors to South Florida's dust season (Prospero, 1999a, 1999b; Prospero et al., 2001; Zuidema et al., 2019). While at least trace amounts of dust are measured nearly every day of boreal summer, extremely high and low (near-zero) dust mass concentrations are episodic. North American dust loading is thought to be more heavily influenced by transport than by emissions, with precipitation playing a nominal role relative to emission and transport (Ridley et al., 2014). Although dust emissions are key importance, episodic SAL releases and the dust concentrations contained within each

SAL are difficult to predict at the subseasonal scale due to the dependence on low-level jets and easterly waves. Here we focus on the transport of a dusty-SAL as opposed to emission. Miami, Florida, is particularly dependent on the characteristics of the lower free-tropospheric winds due to the vast distance the dusty-air must travel and Miami's northern latitude relative to the North African coast where most dust is initially emitted. The goal is to determine the likelihood that dust, once emitted, arrives to South Florida with limited loss to deposition or mixing.

The focus on synoptic, subseasonal, and seasonal dust variabilities will increase the physical understanding of dust movement in the atmosphere and can be applied to improve health warnings and predictions of tropical cyclone development along with shorter-term radiative interactions. First, the in situ dust record is used to quantify key factors for effective dust transport over the Atlantic basin. Second, climatological and synoptic conditions are analyzed to determine the physical mechanisms, which result in the highest downwind dust concentrations. Last, a dust-transport-efficiency (DTE) index is defined to address whether downwind dust concentrations can be predicted on a subseasonal and seasonal time scale.

2. Data and Methodology

In this work we utilize daily in situ dust mass concentration measurements (hereafter referred to as "dust mass") and meteorological reanalysis to find connections between observed dust mass and synoptic-to-seasonal meteorological influences. The daily dust mass record at Miami, Florida, spans a period of 43 years, sufficient length to address daily, subseasonal, and seasonal variabilities. We identify the 15% highest dust concentration days and 15% lowest dust concentrations days measured at Miami to focus our analysis. No filtering was done regarding possible days with tropical storms or hurricanes present in the study area. We utilize National Oceanic and Atmospheric Administration (NOAA)'s transport and dispersion model, Hybrid Single-Particle Lagrangian Integrated Trajectory (HYSPLIT), to visualize air parcel flow to Miami across temporal and spatial scales (Stein et al., 2015). The HYSPLIT runs for the highest and lowest cases allow us to determine the dominate flow regimes resulting in high-dust and low-dust periods. With the relevant meteorological conditions and regions identified, we use the National Centers for Environmental Prediction (NCEP) reanalysis (Kalnay et al., 1996) to find the source of transport variability. Daily data from the NCEP reanalysis is available for the full length of the dust record, which is well accepted, and NCEP files are converted to the HYSPLIT compatible format for the trajectory calculations (Rolph et al., 2017).

2.1. Dust Record

Dust filter data are collected at the Rosenstiel School of Marine and Atmospheric Science campus of the University of Miami located on Virginia Key at 25.7325°N, 80.1632°W, approximately 3 km east of the Florida mainland. Methods for bulk dust mass sampling are unchanged from the Prospero (1999a) protocol, also described in Zuidema et al. (2019). Filter changes occur daily during the boreal summer and biweekly during the remaining months. Strong winds (>5 m/s), extended precipitation events, and occasional tower malfunctions are the sole reason for an irregular filter change. A 10% runtime, equivalent to 2.4 hr, was required of each daily dust sample, following Prospero (1999a). Monthly average values are only considered for months with at least 20 days of samples.

Daily summer dust concentrations are used between 1974 and 2016 with the seasonal average consisting of July and August dust concentrations. July and August receive more dust on average and experience much larger seasonal variability than the other dust-receiving months, May, June, and September, which are not further considered (Table S1 and Text S1 in the supporting information). Annually, July and August contribute 74% (±12%) of the total seasonal dust mass for each year. Since the majority of the dust influx to Miami, Florida, occurs in July and August, which are associated with the largest daily and interannual variability, we focus solely on July and August. In order to highlight the synoptic signal most relevant for episodic high-dust events, we use the 15% percentiles of daily dust mass.

The 15% highest and lowest dust days are considered for each July (346 days total) and August (346 days total) independently across the 43-year time series (Table 1). The lowest 15% threshold includes days with zero dust concentration measured, which is rare for Miami summer. Days with missing data are not included in the calculation. There are 173 days in each high and low composites for July and August, for a total of 692

Table 1
Data Information for July and August Daily Dust Concentration Measurements 1974–2016

	Total days	Missing days	0.0 $\mu g/m^3$	15%	33%	2%
July	1333	175 (13%)	1 (0.08%)	173 High 173 Low	380 High 380 Low	23 High 23 Low
August	1333	180 (13.5%)	4 (0.3%)	173 High 173 Low	380 High 380 Low	23 High 23 Low

Note. The number of missing data days for each month throughout the 43-year time series and the percent of the total number of days (column 3). The number of days with zero dust measured the percent of the total number of days (column 4). The number of high and low days included in threshold selections 15%, 33%, and 2% (columns 5–7).

days considered. The 15% threshold was chosen to represent the greatest deviation from average while maintaining a reasonable sample size. A broader 33% threshold was tested and offered qualitatively similar results of lesser magnitude (Figure S4 in the supporting information). A 2% threshold for the most extreme cases was also tested, which revealed qualitatively similar results, with deviations likely due to the small sample size (Figure S4).

2.2. Trajectory Calculation

HYSPLIT, developed by the NOAA Air Resources Laboratory (ARL), was designed to track pollutants and air mass movements based on a change in position in time from three-dimensional velocity vectors derived from reanalysis or model output (Stein et al., 2015). The backward trajectories are calculated upon a grid of three-dimensional velocity fields derived from a chosen model output or reanalysis (Draxler & Hess, 1998; Stein et al., 2015). Trajectories can be run multiple times per day and at a chosen height (Rolph et al., 2017). A cluster analysis available as part of the HYSPLIT package groups trajectories of similar path by a total spatial variance (TSV). The number of trajectories needed to represent the wind transport environment is determined by the distribution of the TSV: the number of clusters needed is determined by a 30% increase in TSV (Park et al., 2007; Stunder, 1996). The HYSPLIT trajectories utilize the vertical velocity data from the meteorological file. A frequency analysis of the back trajectories, also available through the HYSPLIT package, calculates the percent of trajectories intersecting each grid point divided by the total number of trajectories.

HYSPLIT is used to visualize the circulation preceding each high and low days. In this analysis back trajectories are initialized daily at 25.0°N, 80.0°W, just off the Miami coast to avoid localized land-sea breeze effects and at 2 km in height, above the boundary layer and within the altitude range in which dust is present. Trajectories are run backward for 240 hr (10 days), corresponding to the average time for a dust event to travel from Coastal Africa to the Florida Peninsula. HYSPLIT calculations are done using 6-hourly 2.5° × 2.5° grid NCEP reanalysis files preformatted by the ARL. The use of 6-hourly data over a 10-day period allows us to account for multiple time scales and visualize the circulation. A trajectory for each day of July and August 1974–2016 is begun at 12Z. The cluster and frequency analysis of the trajectories was preformed internally within HYSPLIT, using a 2° grid for the frequency calculation. The back trajectories and analysis aid in identifying what regions are of direct synoptic importance and determine if there are significant differences between the highest and lowest cases.

2.3. Reanalysis Data

The same NCEP 6-hourly wind field that is processed by the ARL for the HYSPLIT trajectory calculations is also used to identify the prevailing circulation patterns. The NCEP reanalysis product from the Earth System Research Laboratory (ESRL) is generated at resolution 2.5° × 2.5° (Kalnay et al., 1996). The current reanalysis spans 1948 to the present with daily coverage. Composites were taken of the 10 days prior to a relevant high- or low-dust measurement in order to diagnose the atmospheric conditions during the transport period (the average transport time for dust to arrive at South Florida from Africa is 10 days). For example, an elevated dust concentration date of 3 August would include a daily average of 25 July to 3 August. Daily mean NCEP files for June, July, and August between 1974 and 2016 were used in analysis, with June data needed due to the backward 10-day average. The analysis shown is an average of 850 and 500mb, representative of the steering flow affecting the SAL. Testing at all levels (850, 700, 600, and 500 mb) individually showed that the flow patterns were consistent at each level and well represented by the layer average (Figure S3). Wind

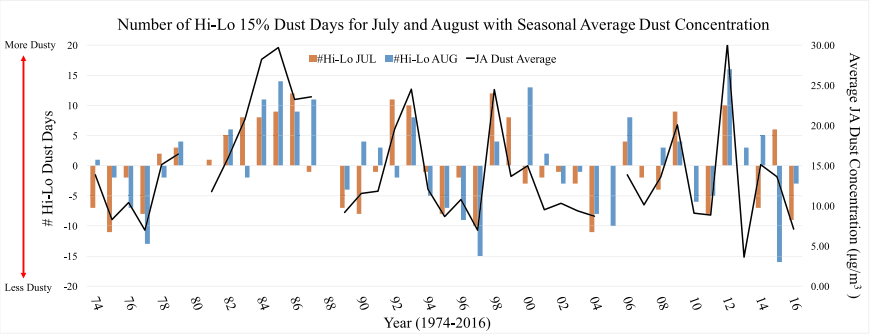

Figure 1. The number of 15% highest minus lowest dust days for July (orange) and August (blue) and the seasonal [July +August] average dust mass (black-line) for each year, spanning 1974–2016.

vectors are depicted long and with curvature ("curly vector"; The NCAR Command Language (Version 6.6.2) [Software], 2019) to better visualize the large-scale flow. The 1,580 geopotential meter contour (gpm) at 850 mb is chosen to represent the horizontal border of the NASH over the North Atlantic based on methods from Li, Li, Fu, et al. (2011).

3. Results

3.1. The High-Low Proxy

The difference between the number of high-dust and low-dust days for July and August for each year, defined using the 15% threshold, is shown in Figure 1. A positive value of "Hi-Lo" days indicates a dustier month and negative value a less dusty month. July and August have the same sign 66% of the years, also showing similar trends in magnitude. July and August Hi-Lo values combined and compared to the average July and August dust mass correlate at $r = 0.89$. We assume that the 15% high-low difference is an indicator of the amount of time Miami is under a distinct dusty regime versus distinct clear regime for each month. This assumption is based on the high correlation between dust mass and the Hi-Lo proxy and consistency between July and August.

This assumption is examined further in Figure 2, in which the July and August 15% highest and lowest dust days are shown by day for each year. Each month is clearly dominated by often consecutive days of high dust or low dust, persistent throughout the month. Easterly wave disturbances carry dusty-air across the Atlantic behind the trough with clear marine-air in the ridge; therefore, it is expected to see multiday events. However, it is unexpected that high-dust days are not followed by low-dust days, but rather each month is

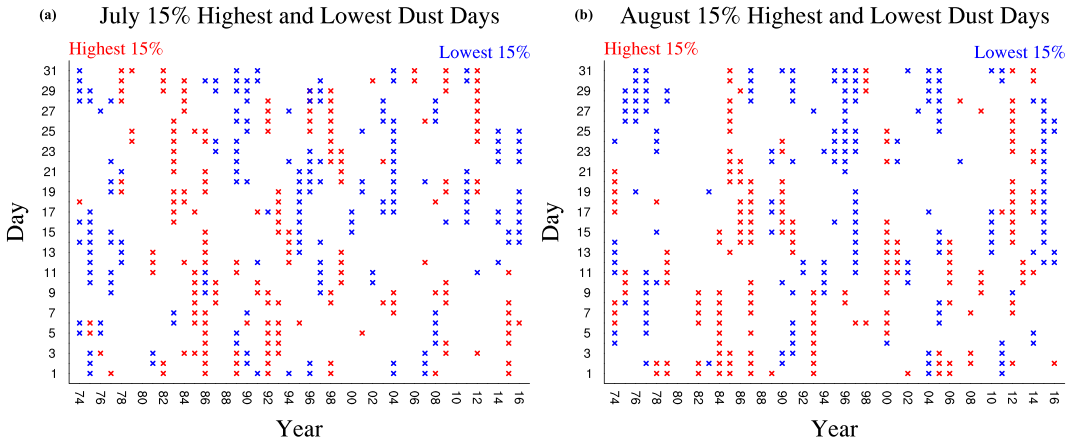

Figure 2. Distribution of 15% highest dust (red) and lowest dust (blue) days measured at Miami, Florida, for (a) July and (b) August by day for 1974–2016.

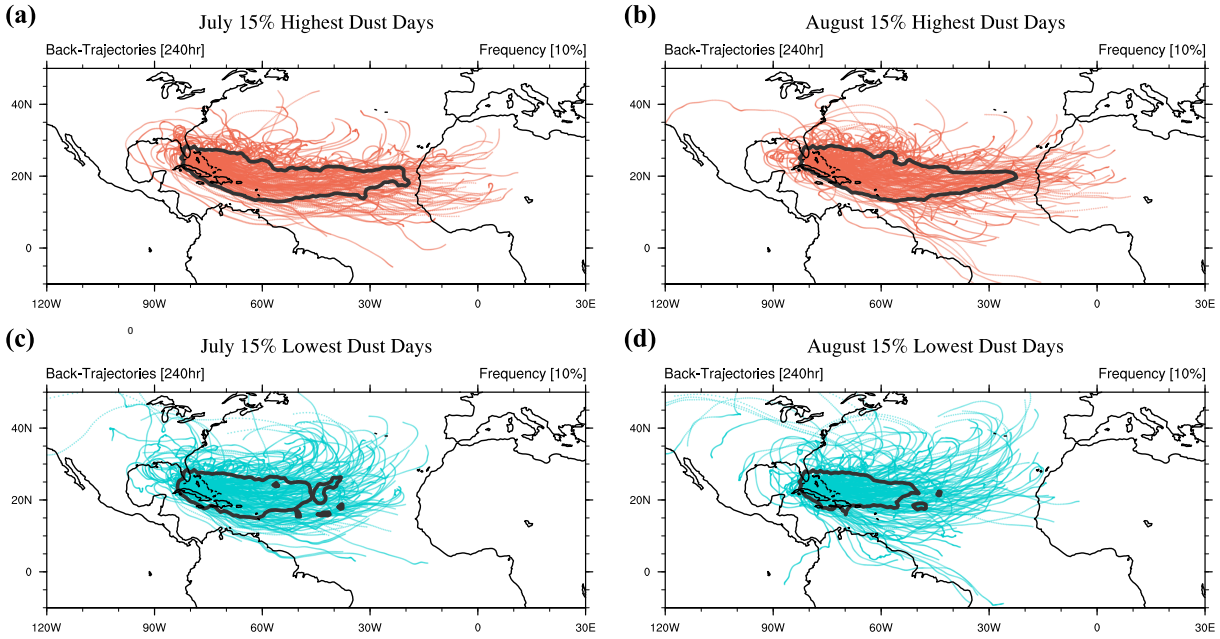

Figure 3. Ensemble of 10-day back trajectories initialized at Miami, Florida, from 2km for the 15% (a and b) highest (pink) and (c and d) lowest (cyan) dust days of July and August from 1974 to 2016. The (black) outline designates the top 10% of grid points with the highest frequency of trajectories passing through.

dominated by either high or low. This suggests a meteorological persistence longer than the typical 5- to 7-day synoptic time scale influences dust loading, not just the easterly waves. Low events can last greater than 10 days, with the longest high event being nine consecutive days. The overall distribution of consecutive-day events is the same for high and low cases and not distinctively different between July and August (Figure S1). Examination of the daily extremes supports our hypothesis that the high-low difference serves well as a proxy for often multiday dusty or relatively dust-free regime, persistent throughout the month.

3.2. Characterization of Transport

The days with the most dust measured at Miami show a distinct transport pathway in which zonal movement across the Atlantic is followed by meridional flow in the Caribbean, in both July and August (Figure 3). The black line encompasses the grid points intersected with the highest concentration of trajectories, representative of the most common flow. The flow is zonal with a northward component after ~60°W, bringing the air parcels northward to Miami. The speed of the westward transport estimated from a traverse of approximately 20 to 80°W in 10 days is 6° per day (Figure 3). Individual trajectories show little meridional movement consistent with reduced mixing with air external to the SAL. Overall, the back trajectories are less spatially variable in July compared to August; however, both are consistent with summertime tropical easterly flow. Cluster analysis for the high-dust cases found two distinct flow regimes based on the total spatial variance distribution: one cluster in which [July: 60% August: 72%] trajectories reach back all the way to Africa (~20°W) and a second cluster [July: 40% August: 28%] following the same path but with a slower east-to-west propagation speed terminating over the Atlantic (~60°W; Figure S2). This indicates that the primary difference may be a difference in the advection velocity or a dusty-air mass lingering over the Florida Peninsula resulting in high concentrations being deposited. The dust load associated with each trajectory averaged for both clusters showed no significant difference in the amount of dust mass brought to Miami by either cluster.

Trajectories for the low-dust cases are much more variable and indicate ways in which high-dust emissions may nevertheless be significantly diluted by the time the dust reaches the western hemisphere. The lowest dust days have no coherent flow across the basin and show multiple flow patterns, evident by the large meridional spread between trajectories. Individual trajectories have large meridional movements indicating mixing of marine and SAL air. The region with the most frequently occurring trajectories spans

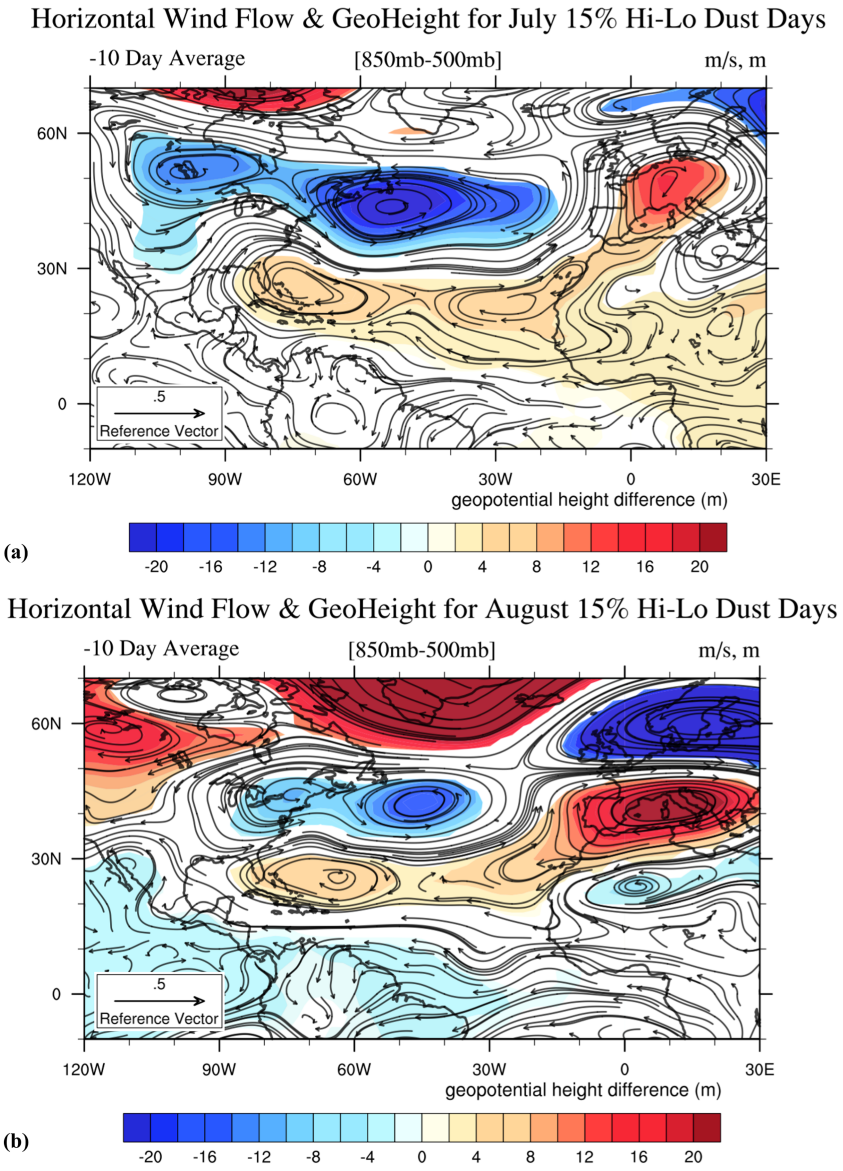

Figure 4. Composite differences in wind vectors and geopotential height between 850mb and 500mb for the 15% highest minus lowest dust days averaged 10 days back for (a) July and (b) August. Shading indicates geopotential height differences with statistical significance over 95%.

approximately 45 to 80°W for the same 10-day period or 3.5° per day compared to the 6° per day for the highest cases (Figure 3). Cluster analysis for the low-dust cases indicates four distinct flow regimes, again based off the total spatial variance distribution (Figure S2). Clusters for July and August do have zonal flow, however, do not reach back to the SAL emission zone. The largest percent of low-dust trajectories originating over the mid-Atlantic [July: 57%, August: 44%] is far west of the SAL ejection zone, and a substantial percent of trajectories [July: 37%, August: 40%] just reaching 30°W but at 30°N, which is north of the SAL ejection region. The remaining clusters flow from the equatorial region [August: 12%] and flow from the continental United States [July: 6%, August: 4%]. The multiple regimes lack a coherent pattern for the lowest dust cases in both July and August and are different than the persistent tropical easterly flow that dominates in high-dust cases.

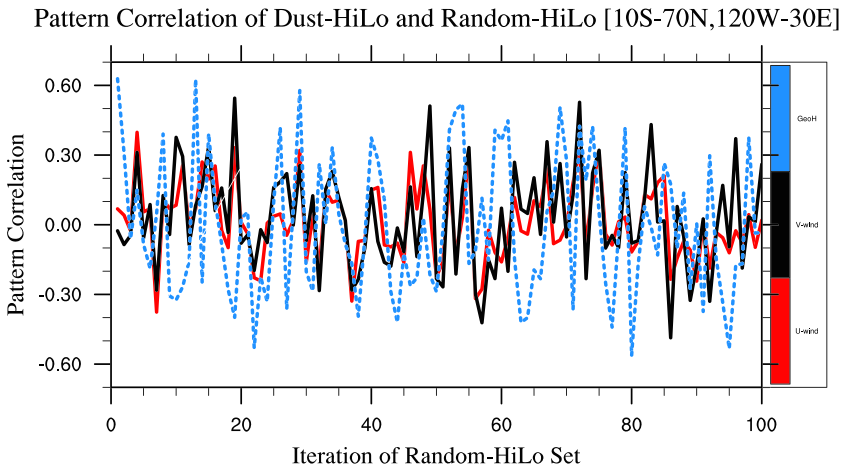

Figure 5. Pattern correlation of 15% dust threshold high-low and random date selected high-low for average geopotential height (blue), zonal wind (red), and meridional wind (black) fields over the North Atlantic region.

3.3. Synoptic Analysis

To attribute the synoptic and climatological conditions that enhance dust transport, the composite differences of geopotential height, zonal wind, and meridional wind for the 15% highest and lowest dust cases are averaged over the preceding 10 days (Figure 4). The average includes the day of the high-dust or low-dust measurement and the 9 days leading up to the event toward representing the full transport time period, from Africa to the Americas. Additionally, the fields of interest are averaged between 850 and 500 mb to capture the full layer that steers and interacts with the SAL prior to intersecting the boundary layer. At each individual layer (850, 700, 600, and 500 mb) the relevant wind and geopotential height anomalies showed 95% significance, based on two-tailed *t* tests, with similar magnitude and pattern, which indicates that the layer average is suitable (Figure S3). The 33% threshold test of zonal wind, meridional wind, and geopotential height showed qualitatively similar features of lesser magnitude, which also surpassed the 95% significance threshold at each level (Figure S4). Additional test was done using the 2% threshold for extreme cases, which also showed increased zonal flow and high-pressure anomaly. The southerly meridional flow was less pronounced in the extreme case but may be due to low sample size (Figure S4).

There is anomalous increased easterly flow in the tropics, especially west of 45°W, and increased northward flow from the tropics along the Florida Peninsula, when dustier conditions occur at Miami (Figure 4). The westerly jet is enhanced at 30°N across the Atlantic basin. There is no significant poleward flow over the Atlantic basin until the Caribbean, as the SAL transport region is dominated by easterlies. The increased anticyclonic flow near Florida is associated with high pressure off the east coast. The anomalous high pressure over Europe and induced pressure gradient between Africa and Europe are consistent with an increased eastward and equatorward flow over North Africa, which may escalate emissions, but would be most relevant prior to the 10-day transport period emphasized here. Anomalous high-low tropical flow is apparent for both July and August (Figure 4) adding confidence that the synoptic regime, increased zonal flow across the tropical Atlantic basin, and increased southerly flow from the Caribbean to the Florida Peninsula are specific to high transport.

A Monte Carlo test was designed to choose dates at random to mimic our 15% dust threshold data set. The 15% dust threshold includes a total of 692 days combining July and August (346 each high and low). At each iteration 692 days were selected at random using a uniform distribution to form a new data set and used in a high-low test for the meteorological fields. The goal of this simulation is to determine whether our findings occur at random ("random-date") or are unique to the dust related days ("dust-date"). We performed a Monte Carlo test for geopotential height, zonal wind, and meridional wind fields. Pattern correlation of between the dust-dates and 100 separate iterations of random-dates depict no defined signal (noise) for all three high-low meteorological fields (Figure 5). The average flow field and geopotential height anomaly of the random-date do not reproduce the anomalies highlighted by the dust data (Figure S5). This test was preformed globally and as a North Atlantic regional subset [10°S–70°N, 120°W–30°E], both showing a wide

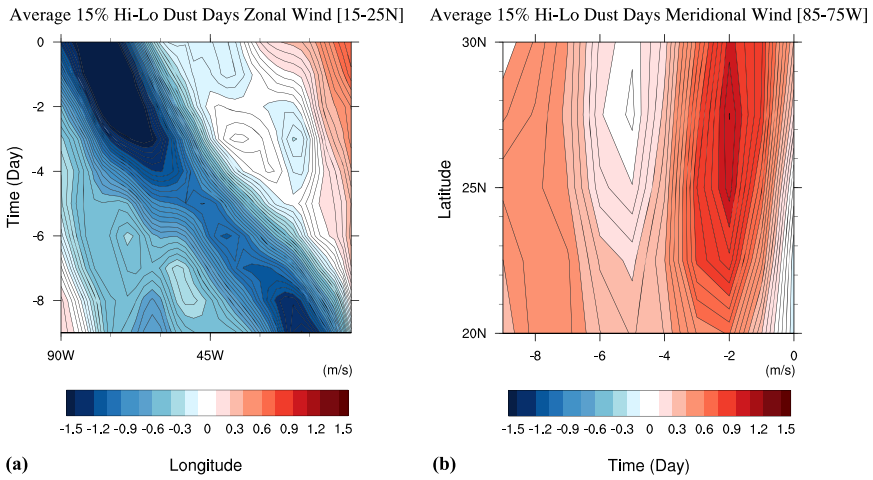

Figure 6. Hovmollers of the (a) zonal wind (b) and meridional wind averaged between 850 and 500 mb for the 15% highest minus lowest dust days by day, extending 10 days previous, for July and August. Miami is located at 25°N, 80°W.

range of inconsistent correlations, or noise. Our findings in Figure 4 are therefore distinctive to the dust-dates.

From the Figure 4 composites, two key regions for favorable dust transport are apparent, northward flow over the Florida Peninsula and a boost of easterly flow at the low latitudes, especially between Florida and 45°W. A time versus longitude plot for tropical zonal winds (Figure 6) shows anomalous strengthening of easterly winds propagating west during high-dust cases, which propagates across the basin. Similarly, a latitude versus time plot for meridional winds over Florida (Figure 6) shows an anomalous burst of northward flow just prior to the high-dust events. July and August are averaged as these showed similar behaviors.

The anomalous wind flow visibly follows the anomalous geopotential height features (Figure 4) warranting further investigation into the atmospheric pressure over the North Atlantic as a source of persistence. To visualize the horizontal extent of the NASH, the most prominent pressure feature in this region, we use 1,580 gpm contours at 850 mb for each high-dust and low-dust cases averaged over the 10-day transport time (Figure 7). The NASH is shifted south and west on average for the highest case comparison to the lowest. The 1,580 gpm contours for high-dust cases are consistently located in close proximity to the Florida Peninsula, where dust is advected north. On average, low-dust cases indicate that the western edge is located over the Atlantic, far from the Florida Peninsula, advecting the dust north over the Atlantic. A portion of the low-dust cases show an extremely western edge of the NASH located over the Gulf of Mexico (Figure 7), advecting dust west of the Florida Peninsula.

For high-dust cases, zonal wind flow is enhanced due to the NASH being in an advantageous position. The anomalous high pressure and increased wind barrier between the westerlies and easterlies result in a corridor effect attributable to a shift in the NASH (Figure 8). Contraction of the NASH and southern displacement leads to a larger gradient between the westerlies and easterlies over the Atlantic; westerlies push toward the equator concentrating the easterly wind band at lower latitudes; this results in overall faster zonal wind speeds (Figure 8). This is supported by Doherty et al. (2008), which showed that westward NASH displacement increases easterly wind and resulting in more dust transport to the Caribbean. The high pressure also provides a defined northern barrier for the SAL: the SAL is advected quickly with little meridional movement. While the tropical wind flow is still the most important mechanism for SAL transport, it is clearly influenced by the NASH.

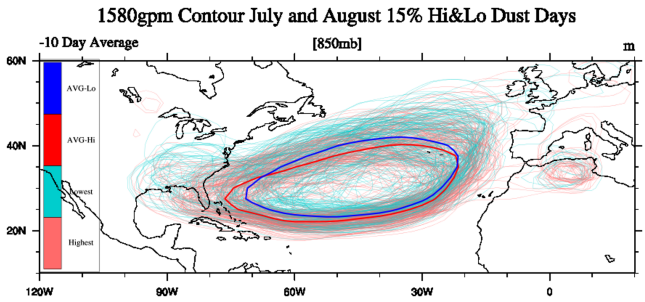

Figure 7. The 1,580 geopotential height meter contours for the 15% highest (pink) and lowest (cyan) dust days averaged ten days back for July and August and the highest average (red) and lowest average (blue).

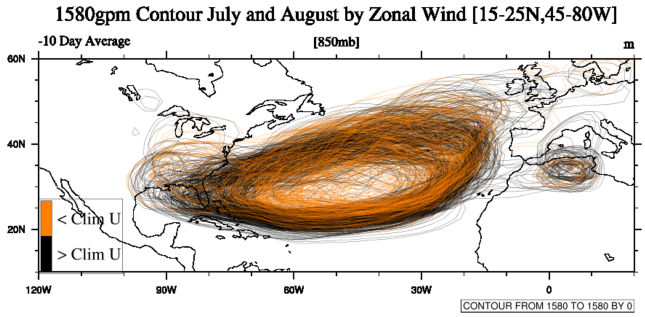

Figure 8. The 1,580 geopotential height meter contours for the 15% highest and lowest dust days averaged 10 days back for July and August. Colors indicate average zonal winds within the [20–30°N, 75–85°W] box greater than average (black) and less than average (orange).

3.4. Dust-Transport-Efficiency (DTE)

We have determined that enhanced easterly movement and northward movement over the Florida Peninsula are crucial for a high-dust event to reach Miami effectively. With the two synoptically significant regions identified, we can develop a simple circulation index to relate with dust concentrations in Miami. This simple calculation can be useful as a subseasonal and seasonal predictor for the likelihood of a high-dust event reaching South Florida, given an emission takes place. DTE index is defined as the hypotenuse of the (i) zonal wind over the Tropical West Atlantic [15–25°N, 45–80°W] and (ii) meridional winds over the Florida Peninsula [20–30°N, 75–85°W] averaged over 850–500mb (Figure 9). Since we use a 850- to 500-mb average, there should be no significance interference from land or mesoscale effects.

The monthly average DTE is calculated using NCEP reanalysis data for July and August of 1974 to 2016 and compared to the high-low difference of the dust days for each year of the Miami dust record (Figure 10). This method is extrapolating the synoptic-scale flow affecting individual events over a subseasonal period, by allowing us to take long-term averages without smoothing over the relevant circulation. There is a stronger correlation in August ($r = 0.38$) than July ($r = 0.30$), which is expected due to the stronger transport dependence. Since transport only accounts for approximately half of dust variability (Ridley et al., 2014), and neither emissions nor precipitation are included in this calculation, the correlations indicate a respectable representation of subseasonal dust loading.

On the subseasonal scale using the DTE is potentially useful, but what about the seasonal scale? July and August monthly mean dust mass concentrations account for an average 74% of the total seasonal dust. Dust events tend to be persistent within both the high- and low-dust years; therefore, the DTE calculation may also be useful as a seasonal dust predictor. The average of August and July DTE is compared directly to seasonal average dust mass in Figure 11. While the overall correlation is low ($r = 0.35$), the maxima and minima track closely. The correlation also changes drastically by decade {1970s ($r = 0.15$), 1980s ($r = 0.46$), 1990s ($r = 0.36$), 2000s ($r = 0.40$), and 2010s ($r = 0.25$)}. This is likely due to the drop in average dust concentration beginning in the 1990s, further evident in the linear trend. The DTE calculation may be less effective as a seasonal predictor but still shows good maxima and minima agreement with seasonal dust.

4. Discussion

High-dust days at Miami, Florida, track back directly to the African coast with a distinct pathway. In both July and August, the highest dust concentrations are associated with a circulation regime of enhanced easterlies across the tropical Atlantic and northward flow at the Florida Peninsula (Figure 3). The high-dust trajectories indicate limited mixing and meridional movement along its path, resulting in large dust quantities remaining aloft. The low-dust days at Miami, Florida, are composed of multiple flow regimes that include relatively weak air movement over the mid-Atlantic, upward flow from the equatorial region, recirculation from the Gulf of Mexico, and flow from the continental United States (Figure 3). Individual low-case trajectories have large meridional movements likely indicating mixing of air masses. Additionally, trajectory vertical motions (Text S2 and Figure S8) show generally slow subsidence for the high cases, which is typical for a SAL. Vertical motions for the low-dust cases (Text S2 and Figure S8) show more trajectory incursion into the boundary layer before reaching Miami and strong vertical ascent, likely attributable to large-scale convection. Since our analysis is based on transport being the largest factor in Miami dust loading, we did not include deposition or precipitation directly in our analysis (Text S3 and Figure S9).

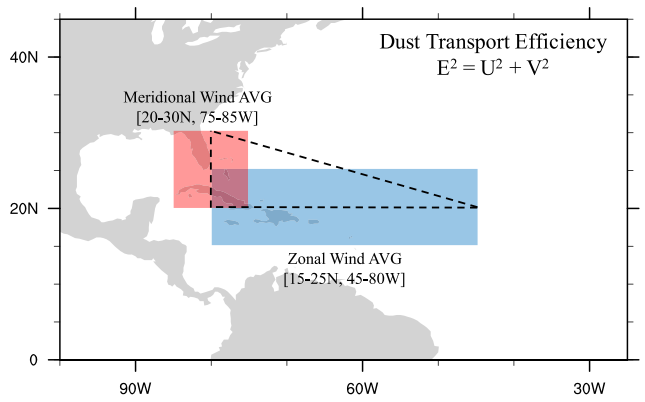

Figure 9. Schematic of dust transport efficiency calculation.

Two key influences for effective dust transport to Miami, Florida, were identified: zonal winds over the Tropical West Atlantic [15–25°N, 45–80°W] and meridional winds over the Florida Peninsula [20–30°N, 75–

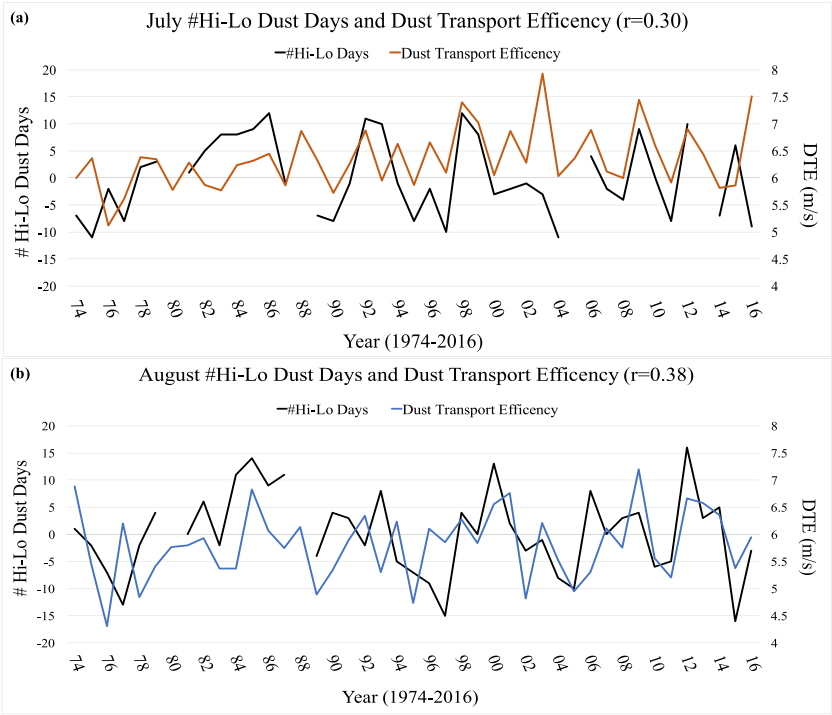

Figure 10. Number of high minus low-dust days (black) and dust transport efficiency (orange, blue) for (a) July and (b) August for 1974–2016.

85°W]. The increased zonal winds and high pressure inhibit the warmer, drier SAL from moving northward and mixing with marine air, while the increased speed also assures a fast transport, with limited time for dust deposition. Once the SAL crosses the Atlantic, the meridional wind core pulls the SAL along the Florida Peninsula at the precisely right location to maximize the dust loading in Miami (Figure 4). The zonal wind clearly propagates across the Atlantic basin for the highest dust cases (Figure 6). Previous work by Karyampudi and Carlson (1988) found that radiative heating from extreme-high concentrations of Saharan dust particles within a SAL led to a strengthening of the midlevel easterly jet while over the ocean. It is possible that high initial emission mass concentration affects the physical transport for the days with the most dust at Miami, by a positive radiative feedback that strengthens the easterly wind flow inside the SAL.

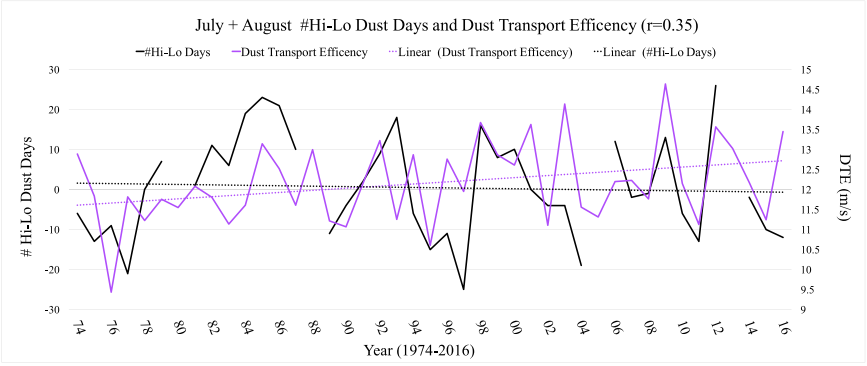

Figure 11. Average dust transport efficiency of July and August (purple) and seasonal [July+August] dust concentration (black) and linear trend (dotted) for 1974–2016.

The winds are enhanced and more favorable over the tropical Atlantic and Florida Peninsula when the NASH is elongated with the western edge in close proximity to the Florida (Figures 7 and 8). When NASH western edge is over the Atlantic, the poleward wind flow occurs over the Atlantic Ocean; far east of the Florida Peninsula, the SAL is dispersed over the Atlantic with minimal dust reaching Miami. Conversely, when the NASH extends extremely west (Figure 7) northward wind-flow occurs in the Gulf of Mexico, the dusty-air is anticipated to be well mixed with the environment and further-aged before reaching Florida, resulting in lower dust concentrations remaining. The western expansion of the NASH also results in a faster burst of easterlies near the FL coast due to the corridor effect (Figure 8). We can attribute the monthly and often seasonal persistence of favorable transport-flow, identified in Figures 1 and 2, to the NASH. Since the NASH is affected by other climate signals, such as NAO or ENSO, this may be the connection to previously found correlations between dust concentrations and climate indices discussed in section 1. High-dust events are also connected to precipitation increase over the Northeast United States and decrease over the Southeast United States consistent with NASH western movement (Text S3 and Figure S9).

The anomalies in zonal wind, meridional wind, and geopotential height are consistent for both July and August, however larger in magnitude for August. This is expected as July is the climatological maxima of dust due to the consistency of summer easterly flow and continuous high emissions. July variations in transport are smaller and most likely offset by the consistently high emissions. August is most highly correlated with annual seasonal dust and more dependent on transport variability then July. Additionally, the NASH is further north in August than July, climatologically (Figure S7 resulting in the southwest NASH positional anomaly having a larger impact, and therefore, has stronger signals.

A DTE index has been defined for Miami (Figure 9), with good subseasonal indication of high-dust concentrations (Figure 10). This method also shows promise for seasonal prediction. This method does not identify actual events but denotes the likelihood that a high concentration dust event will reach the southeast United States if emission occurs. While the correlations [July: 0.3, August: 0.38, JA: 0.35] are moderate, this index is solely dependent on transport wind speeds. With this baseline, we have the potential to develop and add an emission index, and possibly deposition index, to further bolster predictions. Since, to current knowledge, dust forecasts only extend out 120 hr, the possibility of generating a longer-term probabilistic forecast is promising, especially given the abundance of wind forecast data available.

Dust loadings have been decreasing on average at Miami, Florida, since 1974 (e.g., Zuidema et al., 2019); however, the DTE has been increasing (Figure 11). Decreasing dust at long range is consistent with the decreased emissions over the last century seen in observations and climate models (Evan et al., 2006, 2016; Ridley et al., 2014). The increasing DTE indicates that wind speeds have increased in the two key regions possibly attributable to NASH westward movement: W. Li, Li, Fu et al. (2011) and L. Li, Li, and Kushnir (2011) found an intensification and westward shift of the NASH when comparing 1978–2007 to 1948–1977. Furthermore, these studies attribute this western-NASH shift to anthropogenic climate change and suggest that the shift will persist in the future. If the NASH continues to push westward, DTE efficiency will continue to increase, as the proximity to the Florida Peninsula will be more consistent year to year. A climate reconstruction and projection by Evan et al. (2016) found periods of anomalous high- and low-dust emission concentrations {high: 1910s, 1940s, and 1970–1980; low: 1860s, 1950s, and 2000s}. The low- and high-emission periods from the reconstruction match what is seen in the Miami in situ record, high-dust measurements in the 1980s and low in the 2000s. The Evan et al. (2016) study reconstruction and projections also found dust emissions to decrease over the 21st century with anthropogenic climate change, seen as well in the decreasing dust mass concentrations measured at Miami. If emissions continue to decrease with climate change, the overall dust mass at Miami will likely also decrease, despite improved transport. However, if the decadal oscillation pattern, seen in Evan et al. (2016), continues with a new peak in dust emissions, and increasingly favorable transport persists, Miami may get another period of high dust.

5. Conclusions

While this study shows advancement in quantifying the long-range transport of Saharan dust to South Florida, there are many open questions to address. Further investigation and confirmation on the relative dependence of downwind dust concentrations on emission, transport, and wet deposition must be done.

Our study and DTE index are based on the idea that dust loadings at Miami, due to the vast distance from Africa, are chiefly dependent on transport, an idea that is supported by Ridley et al. (2014). It may also prove fruitful to develop a simple circulation index for emissions or a factor for deposition based on precipitation forecasts. Another open question is to what extent dust-radiative feedback help propagate the easterly flow in which the SAL is embedded. Future additional DTE testing will include case studies to determine the success rate the DTE index for individual events in which an emission occurred. In theory, by utilizing forecast model data, we can calculate the DTE index for a given month and construct a probabilistic dust concentration forecast. Furthermore, if a SAL emission occurs, then the forecast data could be used to predict DTE with 10-day lead time, further refining the forecast. However, it is possible that forecast data are unable to predict such subtle changes in wind at long time scales, especially in the low variability tropics. Future work will include utilizing subseasonal forecast model output to test the DTE index as a probabilistic predictor of South Florida dust concentrations at the synoptic, subseasonal, and seasonal timescales.

Acknowledgments
Miami, Florida, dust mass concentration data set is available in netCDF and Excel format at https://doi.org/10.17604/q3vf-8m31. The National Centers for Environmental Prediction (NCEP) reanalysis data, a product provided by the NOAA/OAR/ESRL PSD Boulder, Colorado, USA, are available at https://www.esrl.noaa.gov/psd/data/gridded/data.ncep.reanalysis.html. The HYSPLIT model can be access from https://www.ready.noaa.gov/HYSPLIT.php, a NOAA Air Resource Laboratory product. B. P. K. acknowledges support from DOE DE-SC0019433, NSF OCE1419569 and AGS1558837, and NOAA NA15OAR4320064. We also acknowledge thoughtful and valuable comments by the reviewers.

References

Carlson, T. N., & Prospero, J. M. (1972). Vertical and areal distribution of Saharan dust over the western equatorial North Atlantic Ocean. *Journal of Geophysical Research*, *77*(27), 5255–5265. https://doi.org/10.1029/JC077i027p05255

Chiapello, I., & Moulin, C. (2002). TOMS and METEOSAT satellite records of the variability of Saharan dust transport over the Atlantic during the last two decades (1979–1997). *Geophysical Research Letters*, *29*(8), 1176. https://doi.org/10.1029/2001GL013767

Davis, R. E., Hayden, B. P., Gay, D. A., Phillips, W. L., & Jones, G. V. (1997). The North Atlantic subtropical anticyclone. *Journal of Climate*, *10*, 728–744. https://doi.org/10.1175/1520-0442(1997)010<0728:TNASA>2.0.CO;2

DeFlorio, M. J., Goodwin, I. D., Cayan, D. R., Miller, A. J., Ghan, S. J., Pierce, D. W., et al. (2016). Interannual modulation of subtropical Atlantic boreal summer dust variability by ENSO. *Climate Dynamics*, *46*(1-2), 585–599. https://doi.org/10.1007/s00382-015-2600-7

Doherty, O. M., Riemer, N., & Hameed, S. (2008). Saharan mineral dust transport into the Caribbean: Observed atmospheric controls and trends. *Journal of Geophysical Research*, *113*, D07211. https://doi.org/10.1029/2007JD009171

Doherty, O. M., Riemer, N., & Hameed, S. (2012). Control of Saharan mineral dust transport to Barbados in winter by the Intertropical Convergence Zone over West Africa. *Journal of Geophysical Research*, *117*, D19117. https://doi.org/10.1029/2012JD017767

Draxler, R. R., & Hess, G. D. (1998). An overview of the HYSPLIT_4 modelling system for trajectories, dispersion, and deposition. *Australian Meteorological Magazine*, *47*, 295–308. Retrieved from https://www.arl.noaa.gov/documents/reports/MetMag.pdf

Dunion, J. P., & Velden, C. S. (2004). The impact of the Saharan Air Layer on Atlantic tropical cyclone activity. *Bulletin of the American Meteorological Society*, *85*, 353–365. https://doi.org/10.1175/BAMS-85-3-353

Evan, A. T., Dunion, J., Foley, J. A., Heidinger, A. K., & Velden, C. S. (2006). New evidence for a relationship between Atlantic tropical cyclone activity and African dust outbreaks. *Geophysical Research Letters*, *33*, L19813. https://doi.org/10.1029/2006GL026408

Evan, A. T., Flamant, C., Gaetani, M., & Guichard, F. (2016). The past, present and future of African dust. *Nature*, *531*(7595), 493–495. https://doi.org/10.1038/nature17149

Garrison, V. H., Majewski, M. S., Foreman, W. T., Genualdi, S. A., Mohammed, A., & Simonich, S. L. M. (2014). Persistent organic contaminants in Saharan dust air masses in West Africa, Cape Verde and the eastern Caribbean. *Science of the Total Environment*, *468-469*, 530–543. http://doi.org/10.1016/j.scitotenv.2013.08.076

Ginoux, P., Prospero, J. M., Torres, O., & Chin, M. (2004). Long-term simulation of global dust distribution with the GOCART model: Correlation with North Atlantic Oscillation. *Environmental Modelling & Software*, *19*, 113–128. https://doi.org/10.1016/S1364-8152(03)00114-2

Huneeus, N., Schulz, M., Balkanski, Y., Griesfeller, J., Prospero, J., Kinne, S., et al. (2011). Global dust model intercomparison in AeroCom phase I. *Atmosphere Chemistry and Physics*, *11*, 7781–7816. https://doi.org/10.5194/acp-11-7781-2011

Kalnay, E., Kanamitsu, M., Kistler, R., Collins, W., Deaven, D., Gandin, L., et al. (1996). The NCEP/NCAR 40-year reanalysis project. *Bulletin of the American Meteorological Society*, *77*(3), 437–471. https://doi.org/10.1175/1520-0477(1996)077<0437:TNYRP>2.0.CO;2

Karyampudi, V. M., & Carlson, T. N. (1988). Analysis and numerical simulations of the Saharan air layer and its effect on easterly wave disturbances. *Journal of the Atmospheric Sciences*, *45*(21), 3102–3136. https://doi.org/10.1175/1520-0469(1988)045<3102:AANSOT>2.0.CO;2

Knippertz, P., & Todd, M. C. (2012). Mineral dust aerosols over the Sahara: Meteorological controls on emission and transport and implications for modeling. *Reviews of Geophysics*, *50*, RG1007. https://doi.org/10.1029/2011RG000362

Lau, K. M., & Kim, K. M. (2007). Cooling of the Atlantic by Saharan Dust. *Geophysical Research Letters*, *34*, L23811. https://doi.org/10.1029/2007GL031538

Li, L., Li, W., & Kushnir, Y. (2011). Variation of the North Atlantic subtropical high western ridge and its implication to Southeastern US summer precipitation. *Climate Dynamics*, *39*(6), 1401–1412. https://doi.org/10.1007/s00382-011-1214-y

Li, W., Li, L., Fu, R., Deng, Y., & Wang, H. (2011). Changes to the North Atlantic subtropical high and its role in the intensification of summer rainfall variability in the Southeastern United States. *Journal of Climate*, *24*, 1499–1506. https://doi.org/10.1175/2010JCLI3829.1

Li-Jones, X., & Prospero, J. M. (1998). Variations in the size distribution of non-sea-salt sulfate aerosol in the marine boundary layer at Barbados: Impact of African dust. *Journal of Geophysical Research*, *103*(D13), 16,073–16,084. https://doi.org/10.1029/98JD00883

Mahowald, N., Albani, S., Kok, J. F., Engelstaeder, S., Scanza, R., Ward, D. S., & Flanner, M. G. (2014). The size distribution of desert dust aerosols and its impact on the Earth system. *Aeolian Research*, *15*, 53–71. https://doi.org/10.1016/j.aeolia.2013.09.002

Moulin, C., Lambert, C. E., Dulac, F., & Dayan, U. (1997). Control of atmospheric export of dust from North Africa by the North Atlantic Oscillation. *Nature*, *387*, 691–694. https://doi.org/10.1038/42679

Park, S. K., O'Neill, M. S., Stunder, B. J. B., Vokonas, P. S., Sparrow, D., Koutrakis, P., & Schwartz, J. (2007). Source location of air pollution and cardiac autonomic function: Trajectory cluster analysis for exposure assessment. *Journal of Exposure Science & Environmental Epidemiology*, *17*(5), 488–497. https://doi.org/10.1038/sj.jes.7500552

Prospero, J. M. (1999a). Long-term measurements of the transport of African mineral dust to the eastern United States: Implications for regional air quality. *Journal of Geophysical Research*, *104*(D13), 15,917–15,927. https://doi.org/10.1029/1999JD900072

Prospero, J. M. (1999b). Assessing the impact of advected African dust on air quality and health in the Eastern United States. *Human and Ecological Risk Assessment: An International Journal*, *5*(3), 471–479. http://doi.org/10.1080/10807039.1999.10518872

Prospero, J. M., & Lamb, P. J. (2003). African droughts and dust transport to the Caribbean: Climate change implications. *Science*, *302*(5647), 1024–1027. https://doi.org/10.1126/science.1089915

Prospero, J. M., & Mayol-Bracero, O. L. (2013). Understanding the transport and impact of African dust on the Caribbean Basin. *Bulletin of the American Meteorological Society*, *94*, 1329–1337. https://doi.org/10.1175/BAMS-D-12-00142.1

Prospero, J. M., Olmez, I., & Ames, M. (2001). AL and Fe in PM 2.5 and PM 10 suspended particles in South-Central-Florida: The impact of the long range transport of African mineral dust. *Water, Air, and Soil Pollution*, *125*, 291–317. https://doi.org/10.1023/A:1005277214288

Ridley, D. A., Heald, C. L., & Prospero, J. M. (2014). What controls the recent changes in African mineral dust aerosol across the Atlantic? *Atmosphere Chemistry and Physics*, *14*, 5735–5747. https://doi.org/10.5194/acp-14-5735-2014

Rolph, G., Stein, A., & Stunder, B. (2017). Real-time Environmental Applications and Display sYstem: READY. *Environmental Modelling and Software*, *95*, 210–228. https://doi.org/10.1016/j.envsoft.2017.06.025

Stein, A. F., Draxler, R. R., Rolph, G. D., Stunder, M. D., Cohen, M. D., & Ngan, F. (2015). NOAA's HYSPLIT atmospheric transport and dispersion modeling system. *Bulletin of the American Meteorological Society*, *96*, 2059–2078. https://doi.org/10.1175/BAMS-D-14-00110.1

Stunder, J. B. (1996). An assessment of the quality of forecast trajectories. *Journal of Applied Meteorology*, *35*(8), 1319–1332. https://doi.org/10.1175/1520-0450(1996)035<1319:AAOTQO>2.0.CO;2

The NCAR Command Language (Version 6.6.2) [Software] (2019). Boulder, Colorado: UCAR/NCAR/CISL/TDD. https://doi.org/10.5065/D6WD3XH5

Tsamalis, C., Chédin, A., Pelon, J., & Capelle, V. (2013). The seasonal vertical distribution of the Saharan Air Layer and its modulation by the wind. *Atmosphere Chemistry and Physics*, *13*, 11,235–11,257. https://doi.org/10.5194/acp-13-11235-2013

United Nations Environment Programme (UNEP), World Meteorological Organization (WMO), & United Nations Convention to Combat Desertification (UNCCD) (2016). Global Assessment of Sand and Dust Storms, United Nations Environment Programme, Nairobi. Retrieved from http://uneplive.unep.org/redesign/media/docs/assessments/global_assessment_of_sand_and_dust_storms.pdf

Zhang, H., McFarquhar, G. M., Saleeby, S. M., & Cotton, W. R. (2007). Impacts of Saharan dust as CCN on the evolution of an idealized tropical cyclone. *Geophysical Research Letters*, *34*, L14812. https://doi.org/10.1029/2007GL030225

Zipser, E. J., Twohy, C. H., Tsay, S. C., Thornhill, K. L., Yanelli, S., Ross, R., et al. (2009). The Saharan Air Layer and the fate of African easterly waves—NASA's AMMA field study of tropical cyclogenesis. *Bulletin of the American Meteorological Society*, *90*, 1137–1156. https://doi.org/10.1175/2009BAMS2728.1

Zuidema, P., Alvarez, C., Kramer, S. J., Custals, L., Izaguirre, M., Sealy, P., & Prospero, J. M. (2019). Is summer African dust arriving earlier to Barbados? The updated long-term in-situ dust mass concentration time series from Ragged Point, Barbados and Miami, Florida. *Bulletin of the American Meteorological Society*, *100*(10), 1981–1986. https://doi.org/10.1175/BAMS-D-18-0083.1

References From the Supporting Information

Kelly, P., & Mapes, B. (2011). Zonal mean wind, the Indian monsoon, and July drying in the western Atlantic subtropics. *Journal of Geophysical Research*, *116*, D00Q07. https://doi.org/10.1029/2010JD015405

Sauter, K. S., L'Ecuyer, T. S., van den Heever, S. C., Twohy, C., Heidinger, A., Wanzong, S., & Wood, N. (2019). The observed influence of tropical convection on the Saharan dust layer. *Journal of Geophysical Research: Atmospheres*, *124*, 10,896–10,912. https://doi.org/10.1029/2019JD031365